Low Loss, 3.7GHz Wideband BAW Filters, Using High Power Single Crystal AlN-on-SiC Resonators

Jeffrey B. Shealy, Ramakrishna Vetury, Shawn R. Gibb, Michael D. Hodge, Pinal Patel, Michael A. McLain, Alexander Yu. Feldman, Mark D. Boomgarden, Michael P. Lewis and Rohan Holden
Akoustis Technologies Inc., Huntersville, NC 28078 USA

***Abstract*—Bulk acoustic wave (BAW) filters operating at center frequency of 3.7GHz, comprising of BAW resonators utilizing single crystal aluminum nitride (AlN) piezoelectric films epitaxially grown on silicon carbide (SiC) substrates, are reported. Metal-organic chemical vapor deposition (MOCVD) growth was used to obtain single crystal AlN films on 150-mm diameter c-plane semi-insulating SiC substrates with (0004) X-ray diffraction (XRD) rocking curve full-width half-maximum (FWHM) of 0.025°. The fabricated filters (1.25x0.9 sq.mm) had a center frequency of 3.71GHz and a 3dB bandwidth of 100MHz, an insertion loss of 2.0dB and narrow band rejection of 40dB and out-of-band rejection in excess of 37dB to 8GHz. Individual resonators on the same wafer show an electro-mechanical coupling as high as 7.63% and maximum quality-factors up to 1572. Insertion loss of 5ohm resonators configured as individual 2-port devices changed by 0.15dB after high power survival test at 10W. This is the first demonstration of single crystal AlN-on-SiC based BAW resonator and filter technology at 3.7GHz and illustrates the potential of a single crystal AlN-on-SiC based BAW technology platform enabling compact, high power and high performance filter solutions for high frequency mobile, Wi-Fi and infrastructure applications.**

***Index Terms*—RF Filters, Mobile communication, Piezoelectric devices, Electromechanical devices, Wide band gap semiconductors, bulk acoustic wave resonators, 5G, 4G, LTE, acoustic filters, BAW filters, WiFi, infrastructure.**

I. Introduction

Emerging 5G, Wi-Fi and 4G LTE communication standards require compact, low loss, wide bandwidth filters with steep skirts in mobile and fixed communication devices [1]. The center frequencies of interest for these communication standards extend from traditional bands (below 2.6GHz) to newer LTE frequency bands at 3.4-3.8GHz [1], emerging 5G bands in 3.3-4.2GHz range as well as WiFi between 5 and 6GHz [2] and Citizens Broadband Radio Service [3] in 3.5-3.7GHz range. RF filters for mobile communication devices utilize acoustic resonators which are based on surface acoustic waves (SAW) or longitudinal bulk acoustic waves (BAW). At higher frequencies, SAW filters require smaller width and pitch of the inter-digitated-transducers [4], thus limiting performance.

Film bulk acoustic resonator (FBAR) [5] and solidly mounted resonators (SMR) [6] are the two dominant BAW resonator technologies currently utilized in BAW RF filters due to their small footprint, high Q-factor, high operating frequency, and good power handling. Traditional FBAR and SMR BAW resonators are constructed using thin film piezoelectric AlN materials, deposited by physical vapor deposition (PVD) techniques such as sputter deposition, resulting in poly-crystalline AlN thin film. In contrast, AlN thin films used in this work are epitaxially grown by MOCVD on SiC substrates. SiC substrate is an ideal RF/microwave substrate platform for high performance at high frequency due to its low loss and excellent thermal conductivity [7]. In addition, SiC substrate technology has matured to widespread commercial availability and use of semi-insulating (SI) 6-in SiC and 8-in SI SiC in development [8].

Single crystal AlN films grown by MOCVD on SiC substrates have inherently higher crystal quality compared to poly-crystalline PVD AlN, as evidenced by (0004) X-ray diffraction (XRD) rocking curve full-width half-maximum (FWHM) of 0.025° , compared to typical FWHM of 2-3° in PVD AlN. This improved crystal quality has been shown to result in improvements in acoustic velocity [9] and potentially improved piezoelectric coefficients [10]. Higher longitudinal acoustic velocity in the AlN piezo-material allows thicker materials for the same frequency. It is reported [7] that thermal conductivity of polycrystalline AlN thin films degrades as film thickness decreases, which may constrain the power handling capability of traditional FBAR at higher frequencies.

These factors of improved acoustic velocity, potentially improved piezo-electric coefficients, and improved thermal conductivity suggest that BAW filters constructed using single crystal, epitaxially grown MOCVD-AlN piezo-electric materials offer performance advantages (insertion loss, bandwidth and skirt steepness) over PVD-AlN based BAW filters, especially for high frequency and high power applications.

Prior work [11]–[15] has demonstrated the excellent results using PVD-AlN for higher frequency applications. Prior work using single crystal (MOCVD) Group III-N films for BAW resonators [16]–[20] is summarized in Table 1. In this work, the authors report fabricated filters with a center frequency of 3.71GHz, a 3dB bandwidth of 100MHz, an insertion loss of 2dB and narrow band rejection of 40dB as well as wide band rejection of 35dB extending to 11GHz. To the best of the authors knowledge, this is the first report of filter performance at 3.7GHz, using single crystal AlN-on-SiC based resonators.

II. Device Technology

Single crystal epitaxial piezoelectric layers were grown via conventional MOCVD. The structure comprises aluminum nitride (AlN) of $0.6\mu m$ thickness (nominal target) grown on

TABLE I
SINGLE CRYSTAL GROUP III-NITRIDE BULK ACOUSTIC RESONATORS

Ref.	XRD	Stack	Freq (GHz)	k^2_{eff} (%)	Q_{max}	FOM
[16]	–	GaN/AlN	1.1	5.0	–	–
[17]	0.23°	GaN	6.3	3.4	*1130	38
[18]	0.36°	GaN	2.1	–	*424	–
[19]	2.4°	AlN	3.7	1.1	*1557	17
[20]	0.37°	AlGaN	2.3	4.44	1277	57
This work	0.025°	AlN	3.8	7.63	858	66
This work	0.025°	AlN	3.8	5.87	1572	92

*In this work, Q-factor is calculated from the full mBVD model following [21]. Note [17] [18] [19] quote Q_r which uses only the motional arm of the mBVD model.

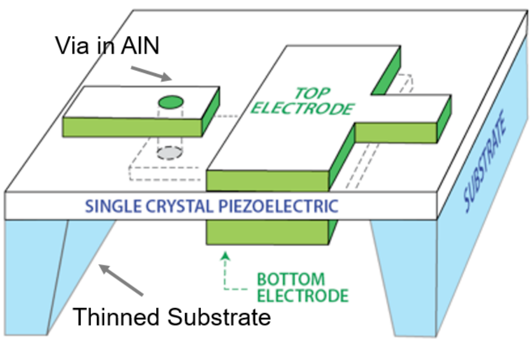

Fig. 1. A schematic diagram of structure of the fabricated resonators, showing top and bottom electrodes on single crystal AlN and a via in AlN to connect to the bottom electrode, situated inside a cavity in a thinned SiC substrate.

$150mm$ diameter, 4H silicon carbide (SiC) substrates. An 8-mask layer, two-sided process wafer process, including sputter-deposited electrode metals and a silicon carbide substrate thinning process yielded resonators with two air interfaces. Backside resonator electrode was routed to the topside of wafer by vias in the AlN thin film. Two resonator device structures are reported in this work, a "baseline" device and a second device, modified to improve Q-factor. A schematic diagram showing the structure of the fabricated resonators is shown in Fig. 1. The measured filter results are obtained from filters constructed using "baseline" resonators.

III. RESONATOR RESULTS

A. k^2_{eff} and Q-factor Characterization

First, the measured (s,y,z)-parameters of the series configured 2-port resonator are mathematically transformed to the (s,y,z)-parameters of the equivalent 1-port. Then, the manifold present between the intrinsic resonator and the measurement probe plane is de-embedded. A plot of the magnitude and phase of the resulting y-parameter for the modified, improved Q-factor resonator is shown in Fig. 2.

The resonant frequency (f_1) and anti-resonant frequency (f_2) were extracted from the zero crossing of phase of the Y-parameter and determined to be 3.673GHz and 3.796GHz for the baseline device and 3.703GHz and 3.796GHz for the modified device, respectively. The calculated value of k^2_{eff}, using eq. (1) was 7.63% and 5.87% for the baseline

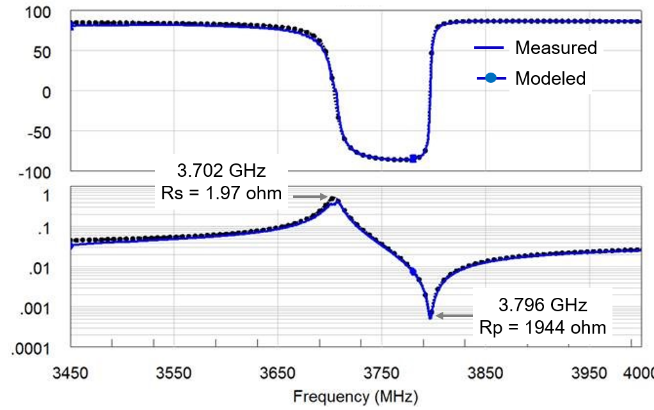

Fig. 2. Measured (de-embedded and transformed to equivalent 1-port) Y-parameter overlaid with mBVD model.

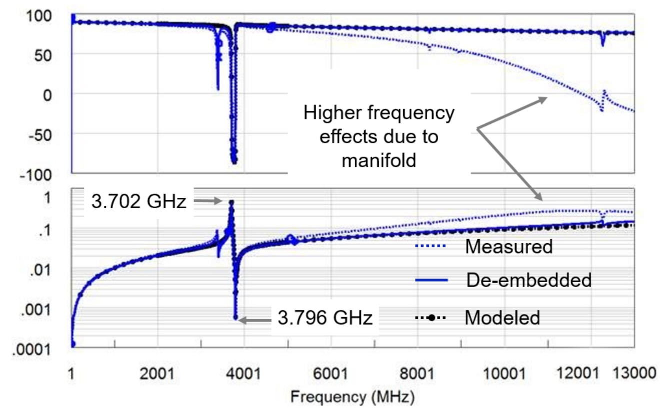

Fig. 3. Comparison of a) measured data without de-embedding, b) measured and de-embedded Y-parameter and c) BVD model fit to the measured and de-embedded Y-parameter.

and modified resonators. Care was taken to ensure that any parasitic inductance in the manifold leading to the resonators was properly de-embedded from the intrinsic resonator. As shown in Fig. 3, parasitic elements present in the manifold leading to the resonator, can cause a second resonance to appear in the measured data.

$$k^2_{eff} = \frac{\pi^2}{4} \cdot \frac{f_1}{f_2} \cdot \frac{f_2 - f_1}{f_2} \qquad (1)$$

A modified Butterworth Van-Dyke (mBVD) model, was fit to the de-embedded y-parameter data. The Q-factor obtained from the fitted mBVD model was evaluated using the method described in [21] and is shown in Fig. 4 for baseline and improved Q-factor resonators.

B. High Power Testing of Single-Crystal Resonator

To investigate the intrinsic power handling capability of single-crystal AlN-on-SIC resonator technology, RF power sweeps were performed on a large area square shaped 5 ohm resonator configured in a discrete 2-port configuration. Using a continuous wave (CW) signal, the input power was linearly swept from +30dBm to +40dBm (in steps of 1dB)

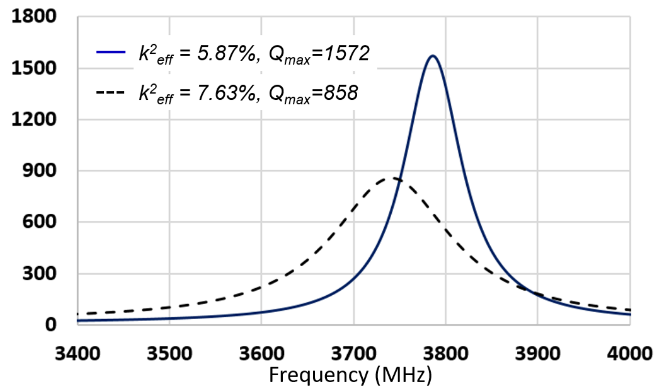

Fig. 4. Q-factor vs frequency, for baseline and modified resonators, based on the mBVD model fit to measured, de-embedded data.

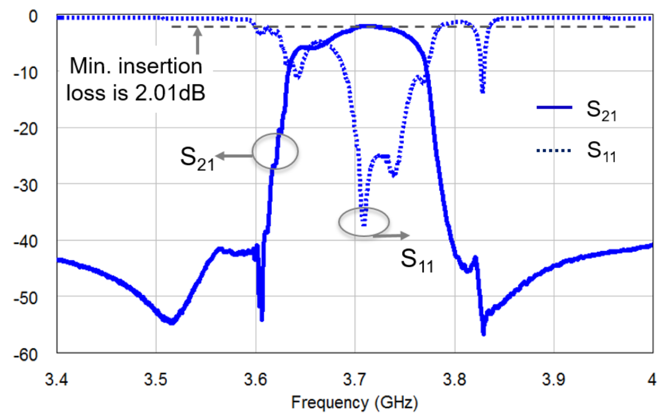

Fig. 5. Measured narrow band S_{21} and S_{11} for the fabricated 3.7GHz filter, showing minimum insertion loss of 2.01dB

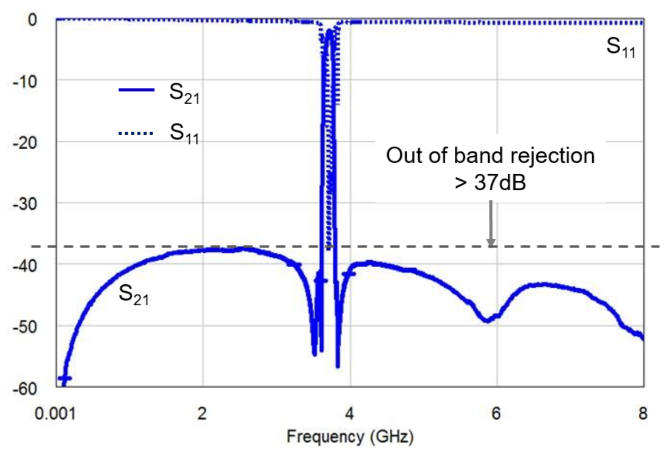

Fig. 6. Measured wide band S_{21} and S_{11} for the fabricated 3.7GHz filter, showing isolation better than 37dB to 8GHz

and the output power was measured to evaluate changes in resonator insertion loss. The maximum input power of the test system was +40dBm and is limited by the power amplifier after the signal generator. The square-configured resonator survived up to 10.1W with only a 0.15dB increase in insertion loss, suggesting that single crystal AlN-on-SiC resonators hold great promise as an enabling technology for compact, low loss, wideband and high power filter solutions at these frequencies.

IV. Filter Results

A 5.5 stage ladder network filter was designed in AWR Microwave Office using the mBVD model of the resonator. The design consisted of 11-elements, including 6-series and 5-shunt resonators. The design was constrained to a symmetrical layout with the series path containing 3 unique resonators and shunt path utilizing 3 unique resonators. A plot of the measured filter response is shown in Fig. 5, showing S_{21} and S_{11} versus frequency. As seen in Fig. 5, the fabricated filter had a center frequency of 3.71GHz and a 3dB bandwidth of 100MHz. The minimum insertion loss was 2.01dB, with an average of 3.04dB across the pass band. The filter displayed excellent narrow band rejection of 40dB as well as wide band rejection of 35dB extending to 8GHz, as seen in Fig. 6. Die size of the fabricated filter was 1.25x0.9 sq.mm.

V. Conclusion

Bulk acoustic wave (BAW) filters operating at center frequency of 3.7GHz, comprising of BAW resonators utilizing single crystal aluminum nitride (AlN) piezoelectric films epitaxially grown on silicon carbide (SiC) substrates are reported. Metal-organic chemical vapor deposition (MOCVD) growth was used to obtain single crystal AlN films on 150-mm diameter c-plane semi-insulating SiC substrates with (0004) X-ray diffraction (XRD) rocking curve full-width half-maximum (FWHM) of 0.025°. The fabricated filters had a center frequency of 3.71GHz and a 3dB bandwidth of 100MHz, an insertion loss of 2.0dB and narrow band rejection of 40dB and out-of-band rejection in excess of 37dB to 8GHz. Realized filter die sizes were 1.25x0.9mm. Individual resonators on the same wafer show an electro-mechanical coupling as high as 7.63% and maximum quality-factors up to 1572. This is the first demonstration of single crystal AlN-on-SiC based BAW resonator and filter technology at 3.7GHz and illustrates the potential of a single crystal AlN-on-SiC based BAW technology platform, enabling small form factor and high power filter solutions for high frequency mobile, Wi-Fi and infrastructure applications.

Acknowledgment

This work was partially supported by National Science Foundation (NSF Award #1556097) and the authors wish to thank Dr. Murali Nair, NSF Program Director, for his continued support of this work.

References

[1] I. Poole, LTE Frequency Bands & Spectrum Allocations, [Online], http://www.radioelectronics.com/info/cellulartelecomms/lte-long-term-evolution/lte-frequency-spectrum.php
[2] http://www.networkcomputing.com/wireless/channel-bonding-wifi-rules-and-regulations/199326059
[3] https://www.fcc.gov/rulemaking/12-354
[4] K. Hashimoto, "RF Bulk Acoustic Wave Filters for Communications" *Artech House.*, pp161-171, 2009

[5] R. Ruby, "Current Status, Future Growth for Filters used in Cell Phones.., *Proc. Intl Symp. on Acoustic Devices*, Chiba, Japan, 2015, pp13-17.

[6] R. Aigner, G. Fattinger, A. Tajic, A. Volatier, F. Dumont, P. Stokes, M. AlJoumayly, "The Edge of Tomorrow in BAW: Innovate, Ramp, Repeat., *Proc. Intl Symp. on Acoustic Devices*, Chiba, Japan, 2015, pp7-12.

[7] S.R.Choi, "Thermal Conductivity of AlN and SiC Thin Films" *Int. Jo. of Thermophysics*, p896, 2006

[8] http://www.iiviadvmat.com/SiC-products/SiC-Products.html

[9] Internal communication.

[10] Y. Ohashi, M.Arakawa, J. Kushibiki, B. Epelbaum, A. Winnacker, Ultrasonic Microscopy Characterization of AlN Single Crystals *Appl. Phys. Express.* 077004 p1-3, 2008.

[11] K.M. Lakin, J.R. Belsick, J.P. McDonald, K.T. McCarron, C.W. Andrus "Thin Film Resonators and Filters, in *Micr. Symp. Digest,IEEE IMS.*, pp1487-1490, 2002.

[12] H.P. Loebl, C. Metzmacher, D.N. Peligrad, "Solidly mounted bulk acoustic wavefilters for the GHz frequency range, in *Proc. IEEE Ultrason. Symp.*, pp919-923, 2002.

[13] T. Nishihara, T. Yokoyama, T. Miyashita, and Y. Satoh, "High performance and miniature thin film bulk acoustic wave filters for 5 GHz, *Proc. IEEE Ultrason. Symp.*, pp969-972, 2002.

[14] R. Lanz, P. Muralt, "Solidly mounted BAW filters for 8 GHz based on AlN thin films, *Proc. IEEE Ultrason. Symp.*, pp178-181, 2003.

[15] G.G. Fattinger, J. Kaitila, R. Aigner, W.Nessler "Thin Film Bulk Acoustic Wave Devices for Applications at 5.2GHz," *Proc. IEEE Ultrasonics Symposium*, p174, 2003

[16] K. Mutamba, D. Neculoiu, A. Muller, G. Konstantinidis, "Micromachined GaN-based FBAR Structures for Microwave Applications, *Proc. of Asia-Pacific Microwave Conf.*, 2006.

[17] A. Muller, et. Al., "6.3GHz FBAR Structures Based upon Gallium Nitride/Silicon Thin Membrane, *IEEE Elec. Dev. Lett.*, Vol. 30, No. 8, pp799-801, 2009.

[18] M. Rais-Zadeh, V. J. Gokhale, A. Ansari, "Gallium Nitride as an Electromechanical Material, *Jour. Micro. Sys.* 23 (6), Dec. 2014.

[19] Y. Aota, Y. Sakyu, S. Tanifuji, H Oguma, S. Kameda, H. Nakase, T. Takagi, K. Tsubouchi "Fabrication of FBAR for GHz Band Pass Filter with AlN Film grown by MOCVD, in *Proc. IEEE Ultrason. Symp.*, pp337-340, 2006.

[20] J.B. Shealy, M.D. Hodge, P. Patel, "Single Crystal AlGaN Bulk Acoustic Wave Resonators on Silicon Substrates with High Electromechanical Coupling," *IEEE Radio Frequency Integrated Circuits Symposium*, May 22-24, 2016

[21] R. Ruby, R. Parker, D. Feld, "Method of Extracting Unloaded Q Applied Across Different Resonator Technologies, *Proc. of IEEE Ultrason. Symp.*, pp1815-1818, 2008